Journal of Power Sources 208 (2012) 18–23

Contents lists available at SciVerse ScienceDirect

Journal of Power Sources

journal homepage: www.elsevier.com/locate/jpowsour

Microbial fuel cell operation with intermittent connection of the electrical load

F. Grondin[a,b], M. Perrier[b], B. Tartakovsky[a,b,*]

[a] Biotechnology Research Institute, National Research Council, 6100 Royalmount Ave., Montréal, Que., Canada H4P 2R2
[b] Departement de Génie Chimique, École Polytechnique Montréal, C.P.6079 Succ., Centre-Ville Montréal, Que., Canada H3C 3A7

ARTICLE INFO

Article history:
Received 23 December 2011
Received in revised form 2 February 2012
Accepted 3 February 2012
Available online 11 February 2012

Keywords:
MFC
External resistance
Intermittent connection
Duty cycle

ABSTRACT

Laboratory-scale microbial fuel cells are often operated with a constant electrical load. Meanwhile, variations in influent strength and quality, as well as the processes of biofilm growth and decay lead to significant changes of the MFC internal resistance over time. This inevitably results in a mismatch between the internal and the external resistances therefore decreasing MFC power output. This study presents the concept of MFC operation with intermittent connection of the electrical load (external resistance). The efficiency of the proposed method is demonstrated by MFC operation with external resistances significantly below the MFC internal resistance and comparing power outputs obtained using either constant or intermittently connected resistances.

1. Introduction

Recent research efforts dedicated to improving microbial fuel cell (MFC) design, materials, and the knowledge of the microbial community have increased MFC power output by several orders of magnitude [1–4]. However, an aspect that has been overlooked is how the produced energy is harvested. MFC power output is maximized when the electrical load (external resistance) connected to the cell is equal to the total internal resistance [5–7]. In laboratory tests, MFCs are often operated with a constant external resistance. Meanwhile, variations in operating conditions and the processes of biofilm growth and decay lead to significant changes of the internal resistance over time. This inevitably results in a mismatch between the internal and the external resistances therefore decreasing MFC power output.

In a laboratory, the resistance mismatch problem can be managed by manually adjusting the variable external resistor connected to the MFC. This method requires a knowledge of MFC internal resistance, which can be estimated in polarization tests [5]. However, the manual external resistance adjustments are infrequent, e.g. weekly or daily, while the internal resistance could significantly change within minutes, thus leading to significant energy losses. Recently, Woodward et al. [8] proposed a method for external resistance control, which uses an on-line perturbation/observation (P/O) algorithm for maximizing the power output. Also, a logic-based control approach for adjusting the external resistance was recently proposed [9]. Both methods provide real-time optimization of the external resistance, however the practical implementation of these methods would require a device with a controllable electrical load. Meanwhile, the electrical loads are not always controllable.

When controlling electrical motors and other electrical devices, the average applied power is often controlled by periodically turning on and off the switch between the supply and the load. This mode of operation is described by a duty cycle, defined as a portion of time during which the power source is connected to the device. The duty cycle can be used to adjust the electrical load and match the resistances (impedances). A similar approach is often used in maximum power point tracking systems for efficient harvesting of renewable energy [10,11] where a converter is introduced between the power source and the device. In this case the duty cycle is used to adjust the load and match the impedances. Indeed, the converter can be seen as an equivalent resistance added to the non-controllable electrical load with the value of this equivalent resistance being a function of the duty cycle.

The approach of controlling the equivalent resistance by duty cycle adjustment could be also used in MFC operation, however it requires a thorough evaluation, since the performance of the electricigenic microorganisms under a varying electrical load is unknown. This study presents the concept of MFC operation with intermittent connection of the electric load (*R*-periodic operation) and describes the experimental results, which confirm the efficiency of the proposed method.

* Corresponding author. Tel.: +1 514 496 2664; fax: +1 514 496 6265.
E-mail address: Boris.Tartakovsky@nrc-cnrc.gc.ca (B. Tartakovsky).

0378-7753/$ – see front matter.
doi:10.1016/j.jpowsour.2012.02.010

2. Materials and methods

2.1. Analytical methods, inoculum, and media composition

Acetate concentration in the anodic liquid was analyzed on an Agilent 6890 gas chromatograph (Wilmington, DE, USA) equipped with a flame ionization detector. Method details are provided in Tartakovsky et al. [12].

The MFC was inoculated with 5 mL of anaerobic sludge with a volatile suspended solids (VSS) content of approximately 40–50 g L^{-1} (Lassonde Inc., Rougemont, QC, Canada) and 20 mL of effluent from an operating MFC.

The nutrients solution was composed of (in g L^{-1}): yeast extract (0.8), NH_4Cl (18.7), KCl (148.1), K_2HPO_4 (64.0), and KH_2PO_4 (40.7) and sodium acetate. The concentration of sodium acetate in the nutrients solution was varied between 10 or 40 g L^{-1} (as CH_3COO^-) in order to obtain the desired organic load. One mL of a trace elements stock solution was added to 1 L of deionized water, which was fed to the MFC. The stock solution composition is provided in [13]. The anodic liquid solution conductivity was 16–18 mS cm^{-1}.

2.2. MFC design and operation

A membrane-less air-cathode MFC was constructed using nylon plates. The anode was made of 5 mm thick carbon felt measuring 10 cm × 5 cm (SGL Canada, Kitchener, ON, Canada) and the cathode was a gas diffusion electrode with a Pt load of 0.5 mg cm^{-2} (GDE LT 120EW, E-TEK Division, PEMEAS Fuel Cell Technologies, Somerset, NJ, USA). The electrodes were separated by a nylon cloth with a thickness of about 0.5 mm. An external recirculation loop was used for anodic liquid mixing (Fig. 1). The anodic chamber temperature was maintained at 25 °C. The MFC was continuously fed with the acetate stock solution and a trace metals solution. A hydraulic retention time of 5 h was maintained.

Intermittent connection of an external resistor (R_{ext}) to MFC terminals was achieved by adding an electronic switch (IRF540, International Rectifier, El Sequndo, CA, USA) to the external electrical circuit (Fig. 1). The switch was computer-controlled using a Labjack U12 data acquisition board (LabJack Corp., Lakewood, CO, USA). The data acquisition board was also used to record MFC voltage.

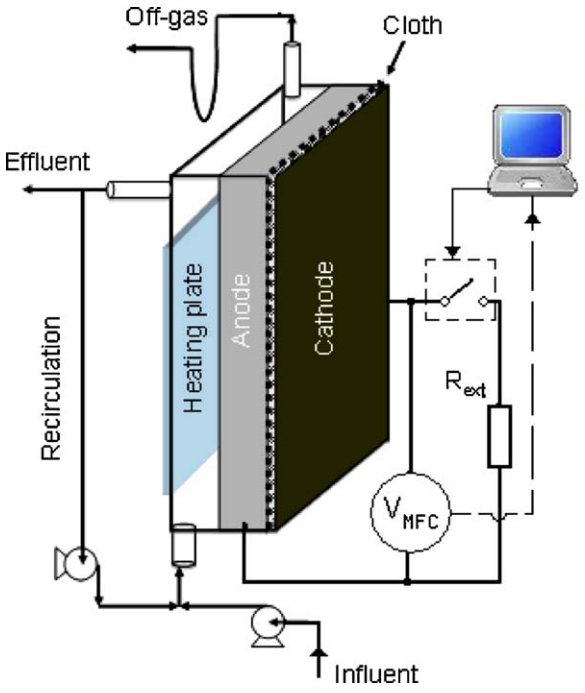

Fig. 1. Schematic diagram of the experimental setup.

MFC operation with intermittent connection of an electrical load can be described by a duty cycle (D) as:

$$D = \frac{t_{on}}{t_{off} + t_{on}} \quad (1)$$

where t_{on} is the "on" time within each cycle during which the electrical load (external resistance) is connected and t_{off} is the disconnection ("off") time. The cycle time (T_{cyc}) can be expressed as $T_{cyc} = t_{on} + t_{off}$.

MFC operation with an adjustable duty cycle was achieved by switching between an "on" and an "off" states based on voltage measurements at MFC terminals (U_{MFC} in Fig. 1). The following algorithm was used. R_{ext} was disconnected, if U_{MFC} decreased below a pre-defined minimum voltage threshold (U_{min}), then R_{ext} was re-connected once U_{MFC} exceeded a predefined maximum voltage threshold (U_{max}).

2.3. Electrochemical measurements and performance characterization

Polarization tests (PTs) were carried out to estimate the total internal resistance (R_{int}) of the MFC. In each PT, R_{ext} was disconnected for 30 min, then open circuit voltage (OCV) was measured. Subsequently, the external resistance was re-connected and stepwise decreased every 10 min from 1000 Ω to 5–15 Ω to obtain 7–10 measurements. Voltage (U) was measured at the end of each 10 min period. Stable voltage readings were assured by comparing voltage values during the last 3 min of each period. The resulting voltage and current values were used to construct polarization curves, i.e. voltage vs. current plots from where the MFC's total (ohmic and solution) R_{int} was estimated by the slope of the linear region [14].

During MFC operation with constantly connected R_{ext}, power output (P_{out}, mW L_A^{-1}) was calculated using measurements of output voltage and a known value of R_{ext}. During MFC operation with intermittently connected R_{ext} an average power output per cycle (P_{av}) was calculated as

$$P_{av} = \frac{1}{T_{cyc}} \int_0^{T_{cyc}} \left(\frac{U^2(t)}{R_{ext}} \right) dt \quad (2)$$

where $U(t)$ is the voltage measured at R_{ext} at time t. The data acquisition board measured the voltage with an interval of 50 ms corresponding to at least 20–30 measurements per cycle, which were then used for the P_{av} calculation.

The apparent total internal capacitance of the electrode surface was estimated by analyzing cyclic voltammograms obtained at different sweep rates [15]. Cyclic voltammetry was performed using an electrochemical analyzer CHI 601A (CH Instruments, Austin, TX). A two-electrode setup was used (anode as a working electrode and a cathode as a counter and reference electrode). Also, the measurements were repeated with the cathode as a working electrode and the anode as a counter and reference electrode. The voltammograms were performed around the OCV value estimated as described above at scan rates between 1 and 15 mV s^{-1}. Current measurements at a voltage corresponding to MFC OCV were plotted against the scan rate and the apparent internal capacitance was estimated as a slope of the linear part of this curve.

2.4. Factorial design experiment

Two full factorial plans aimed at optimizing P_{av} were performed by varying the periodic operation voltage threshold (U_{min} and U_{max}) between low, intermediate and high values. These plans necessitated 9 different trials each.

Table 1
Three-level factorial design test at R_{ext} = 10 Ω.

Run	U_{max} (V)	U_{min} (V)	P_{av} (mW)
1	0.32	0.13	1.61
2	0.32	0.132	1.59
3	0.32	0.134	1.62
4	0.35	0.13	1.49
5	0.35	0.132	1.33
6	0.35	0.134	1.41
7	0.38	0.13	1.46
8	0.38	0.132	1.27
9	0.38	0.134	1.13
10	0.35	0.132	1.44
11	0.35	0.132	1.48

The first experiment used a 10 Ω external resistance, and contained 3 additional center points to assess measurements variability. Design values of the factors for this experiment are given in Table 1. The second plan used a 5 Ω external resistance and the voltage thresholds were adjusted accordingly, since a lower resistance usually implies lower voltage. U_{min} and U_{max} values selected for this experiment are provided in Table 2.

3. Results and discussion

3.1. Internal resistance and capacitance estimations

Several polarization tests were conducted to estimate the MFC internal resistance, both during MFC operation at a "normal" organic loading rate (OLR) of 4 g L_R^{-1} d^{-1} (corresponding to 1000 mg L^{-1} influent concentration) and at a "low" OLR of 1 g L_R^{-1} d^{-1} (250 mg L^{-1} influent concentration). The corresponding acetate concentrations in the anodic chamber were 170–200 mg L^{-1} and 20–40 mg L^{-1}, for normal and low OLRs, respectively.

At a normal OLR, R_{int} estimations varied between 19 and 24 Ω, as can be seen from Fig. 2A, which shows three separate polarization tests. These estimations are in agreement with an external resistance of 18–25 Ω used during MFC operation by the computer-controlled perturbation/observation algorithm, which maximized MFC power output by real time external resistance correction [6,13].

MFC operation at a reduced organic load led to an increase of R_{int} to 50–70 Ω, as can be seen from the analysis of the polarization curves shown Fig. 2A. Also, acetate limitation led to a power output decrease from 2.1 ± 0.2 mW to 0.8 ± 0.1 mW. Overall, the polarization tests demonstrated a strong dependence of R_{int} on the carbon source concentration in the anodic chamber. A similar dependence was observed in a MFC fed with synthetic wastewater [13].

Estimation of an MFC's apparent capacitance was carried out using the cyclic voltammetry (CV) technique. After cyclic voltammograms were obtained at different scan rates, the current in the middle of the potential range was plotted as a function of the sweep rate to estimate the slope, as shown in Fig. 2B. The cyclic voltammograms were acquired at OLRs of 4 and 1 g L_R^{-1} d^{-1} and apparent capacitance estimations of 0.20 ± 0.08 F and 0.20 ± 0.09 F, were obtained for normal and low OLRs, respectively. Although the apparent capacitance estimations obtained by cyclic voltammetry have a number of known limitations and can be biased [15], the estimations pointed out to a significant internal capacitance of the MFC. This capacitance might be attributed to the high surface area of the carbon felt anode [16].

Table 2
Three-level factorial design test at R_{ext} = 5 Ω.

Run	U_{max} (V)	U_{min} (V)	P_{av} (mW)
1	0.32	0.085	1.37
2	0.345	0.085	1.28
3	0.37	0.085	1.22
4	0.32	0.1025	1.37
5	0.345	0.1025	1.20
6	0.37	0.1025	1.00
7	0.32	0.120	1.83
8	0.345	0.120	1.29
9	0.37	0.120	1.09
10	0.345	0.1025	1.17
11	0.345	0.1025	1.06
12	0.345	0.1025	1.27

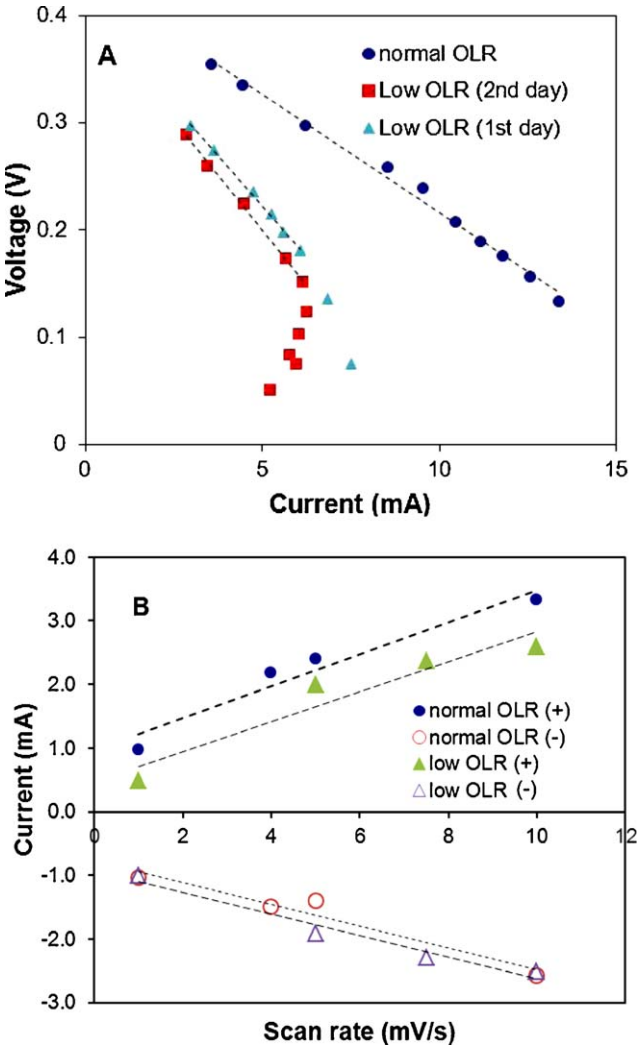

Fig. 2. (A) polarization curves and (B) current vs. scan rate diagrams obtained under normal OLR (4 g L_R^{-1} d^{-1}) and low OLR (1 g L_R^{-1} d^{-1}) conditions. R_{int} estimations were 22, 41, and 38 Ω for normal OLR, low OLR (day 1) and low OLR (day 2) tests respectively. Apparent capacitance estimations were 0.20 ± 0.08 F and 0.20 ± 0.09 F for normal and low OLR, respectively. "+" corresponds to anode as a working electrode.

3.2. R-periodic MFC operation

Recently, Donovan et al. [17] proposed an MFC power management system, which included a capacitor for energy accumulation and a DC–DC converter. This system was operated by accumulating the electrical energy in the capacitor for several dozens of minutes and then dispensing it in a burst of high power. This approach, however, did not address the problem of MFC operation at external resistance (impedance) values, which are significantly lower than the MFC internal resistance.

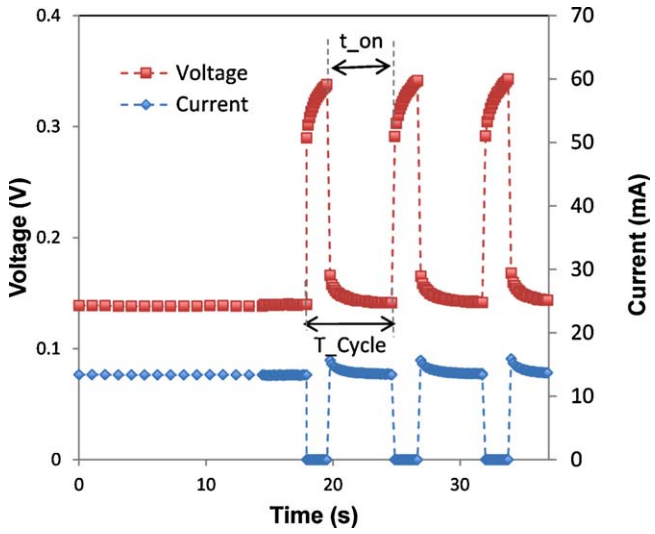

Fig. 3. MFC operation with intermittent resistance connection (R_{ext} = 10 Ω).

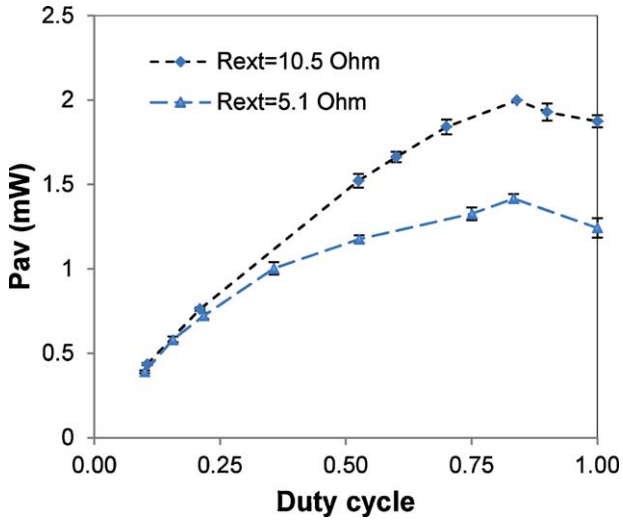

Fig. 4. Average power output as a function of the duty cycle at R_{ext} = 10.5 Ω and R_{ext} = 5.1 Ω. Each data point represents an average of 6 values measured after at least 8 h of MFC operation for R_{ext} = 10.5 Ω and 1 h of MFC operation for R_{ext} = 5.1 Ω.

Here, we hypothesized that the considerable internal capacitance of the MFC can be used to resolve the resistance mismatch problem by MFC operation with periodic connection and disconnection of the electrical load (external resistance) at a relatively high frequency. The proposed method of MFC operation was tested with R_{ext} = 10 Ω, which was chosen to be below the estimated internal resistance of 19–24 Ω. The connection (t_{on}) and disconnection (t_{off}) times were set to 5 s and 2 s, respectively. The test was carried out under acetate non-limiting conditions (i.e. OLR = 4 g L_R^{-1} d^{-1}). Fig. 3 shows a one cycle snapshot of MFC voltage (U_{MFC}) measured at the electrode terminals and the current at R_{ext}, calculated as $I_{ext} = U_{ext}/R_{ext}$, where U_{ext} is the voltage measured at the resistor terminals. During the t_{off} part of each cycle R_{ext} is disconnected (zero current) and U_{MFC} increases. During the t_{on} part of the cycle R_{ext} is re-connected and U_{MFC} exponentially decreases approaching about 0.14 V by the end of the cycle. An average (per cycle) power is calculated with respect to both parts of the cycle according to Eq. (2). In the test presented in Fig. 3, a P_{av} value of 1.73 ± 0.03 mW was obtained. This value was less than the steady state power output of 2.1 mW obtained with a constantly connected 20 Ω resistance, because of non-optimal cycle parameters. Nevertheless, the test demonstrated that by periodically connecting and disconnecting R_{ext} a MFC could be operated without significant losses in power output even at R_{ext} values below R_{int}.

3.3. D-curves and factorial design tests

Power output obtained during MFC operation with periodic connection of R_{ext} might depend on the choice of cycle parameters (t_{on} and t_{off}), which define the duty cycle value. To study the impact of D on MFC power output the MFC was operated at several D values using a 10 Ω external resistance. For this test a constant value of t_{on} = 3 s was used, while t_{off} was varied to obtain different D values. Fig. 4 shows the impact of D on the average (per cycle) power output. Data points in this curve were obtained by MFC operation at each D value for 8–12 h. A clear optimum was observed at D values between 0.75 and 0.95. P_{av} was maximized at t_{on} = 3 s and t_{off} = 0.6 s. Notably, a P_{av} value of 2 mW obtained at these cycle settings was quite close to 2.1 mW measured with a constantly connected 20 Ω resistor. The D-curve was also acquired at R_{ext} = 5 Ω with t_{on} = 1 s. In this test P_{av} was estimated after 1 h at each D setting. A similar trend was observed, although power output was lower (Fig. 4). We hypothesize that P_{av} could be improved by using shorter cycles (i.e. increasing the frequency), but because of hardware limitations we were unable to carry out this test. At t_{off} values below 0.1 s the number of voltage samples was insufficient for an accurate estimation of P_{av}.

Additional optimization of cycle parameters (t_{on} and t_{off}) was performed using the factorial design experiment. For practical purposes it was decided to switch between the "on" and "off" periods of each cycle by using voltage measurements rather than the preselected length of t_{on} and t_{off}. Indeed, voltage profiles in Fig. 3 always decrease during the t_{on} part of the cycle until reaching a steady state value. Thus, "on" (resistor is connected) part of the cycle can end if voltage decreases below a pre-set minimum threshold value (U_{min}). When R_{ext} is disconnected the voltage increases until approaching the OCV value. A pre-set maximum voltage threshold (U_{max}) can be used to end the "off" (disconnected R_{ext}) part of the cycle. The optimal U_{min} and U_{max} values were estimated in the full factorial design experiments.

The first factorial design experiment was carried out at a R_{ext} = 10 Ω and an OLR of 4 g L_R^{-1} d^{-1}. U_{min} and U_{max} values (factors) used in this test are given in Table 1. The response surface (Fig. 5A) was approximated using a second-order regression model. Statistical analysis of the regression coefficients showed that only linear interactions of the factors should be included. The resulting model had a R^2_{adj} of 0.87 and a p-value of 0.94, i.e. the model was adequate. The optimal operating point was found at a U_{max} = 0.32 V and U_{min} = 0.134 V. This corresponds to a low U_{max} and a high U_{min} boundary, i.e. shorter cycles are preferable. This conclusion is consistent with our initial analysis suggesting that shorter cycles lead to optimal power production.

In the full factorial experiment using a R_{ext} of 5 Ω, the voltage thresholds were adjusted to assure cycles of reasonable duration (Table 2). The response function obtained in this test is shown in Fig. 5B. Once again, a regression model with linear interactions of the factors described the response surface with a sufficient accuracy (R^2_{adj} = 0.86, p-value = 0.64). The optimal operating point was found at U_{max} = 0.32 V and U_{min} = 0.12 V. Overall, the optimal threshold values provided reasonable cycle time and guaranteed MFC operation in a range of output voltages suitable for operating an electronic device, e.g. an up-converter.

3.4. R-periodic operation under varying organic load

Estimation of R_{int} at "normal" and "low" OLRs demonstrated a significant increase of R_{int} under carbon source – limiting

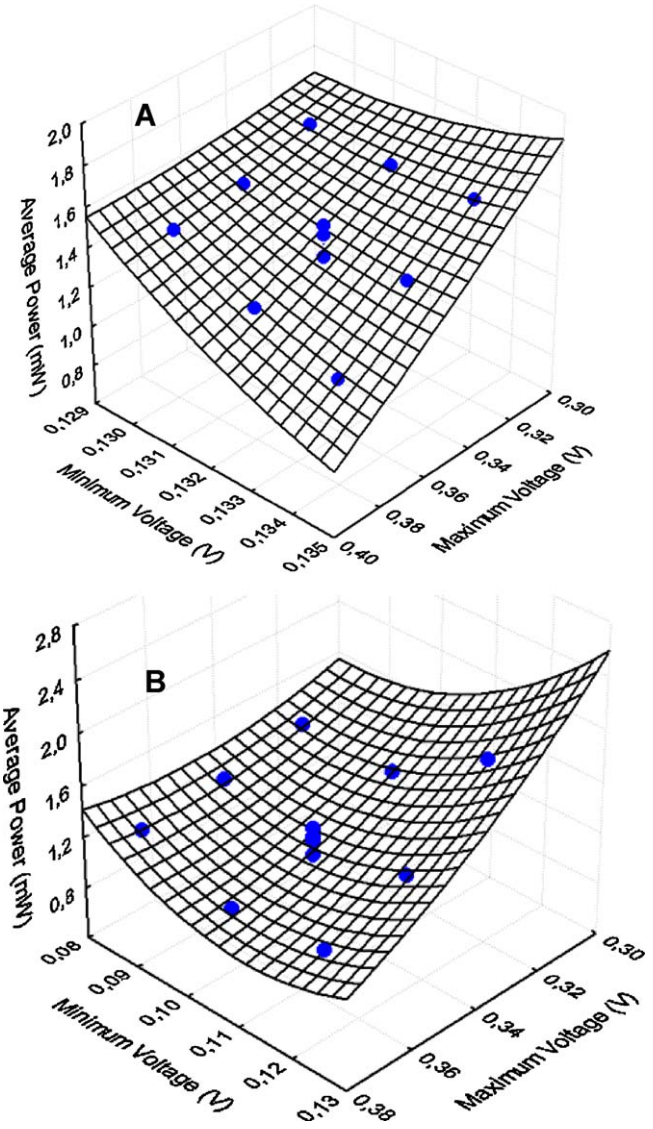

Fig. 5. Response surfaces obtained in 3-level factorial design tests performed at R_{ext} = 10.0 Ω (A) and at R_{ext} = 5.0 Ω (B).

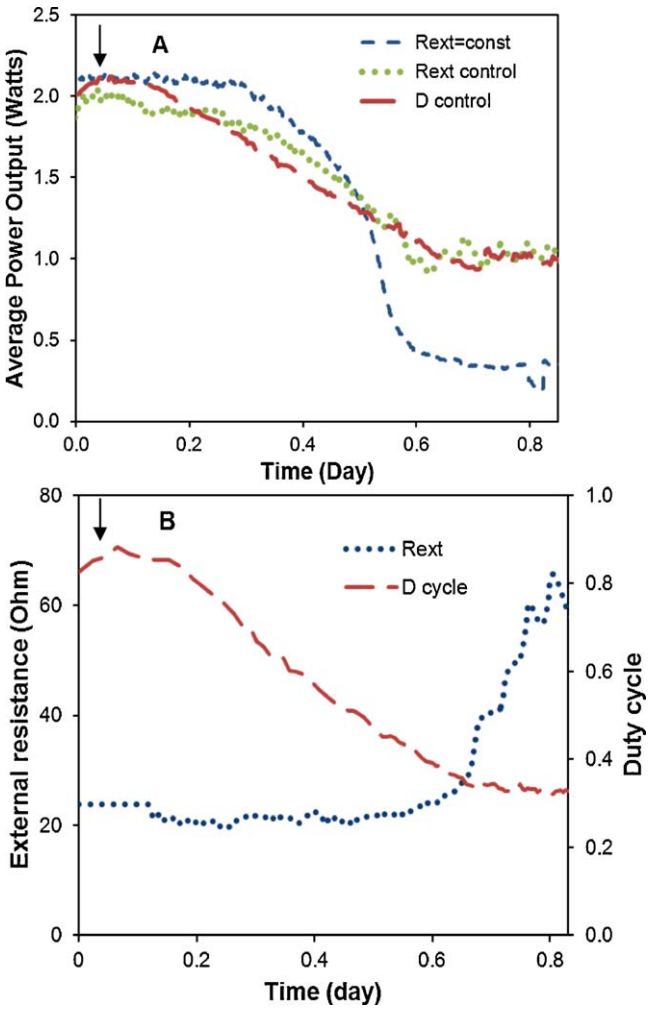

Fig. 6. Average power output (A) and R_{ext} or duty cycle values (B) during organic load perturbation. MFC was operated either with a constant R_{ext} = 20 Ω, or with the P/O algorithm for R_{ext} control, or with intermittent connection of R_{ext} = 10 Ω. The arrows indicate the OLR change from 4 to 1 g L_R^{-1} d^{-1}.

conditions. This change of R_{int} requires electrical load to be adjusted in order to avoid MFC operation at R_{ext} values significantly below the R_{int} value and, consequently, a loss of power output [8,13]. MFC operation with periodic connection of R_{ext} enables MFC operation at R_{ext} values below R_{int}. Furthermore, duty cycle control based on voltage measurements, as described above, provides a real-time algorithm for maximizing MFC power output.

The robustness of the proposed approach was tested in a MFC, which was first operated with an acetate load of 4 g L_R^{-1} d^{-1} followed by a transition to 1 g L_R^{-1} d^{-1} to create carbon source – limiting conditions. This test was repeated several times, each time using a different method for controlling R_{ext}. Throughout the first test, R_{ext} was kept at 20 Ω. This choice of R_{ext} maximized power output at acetate non-limiting conditions, however a drop in P_{av} was observed as soon as acetate concentration in the anodic liquid declined (Fig. 6A). Furthermore, an attempt to change R_{ext} to 10 Ω during the acetate-limiting phase resulted in an even lower power output (Fig. 6A, a 10 Ω operation at around 0.8 day).

During the second test the same acetate load profile was used, while the external resistance was controlled by the P/O algorithm described in Woodward et al. [8]. Real-time optimization of R_{ext} led to a higher power output at low OLR (Fig. 6A). R_{ext} chosen by the P/O algorithm was at around 20 Ω under acetate non-limiting conditions, while it increased to 50–70 Ω during the acetate-limiting phase of the test (Fig. 6B). Notably, the P/O algorithm required R_{ext} to be adjusted every minute to track the changes in R_{int}.

In the third test the MFC was operated with an intermittently connected R_{ext} of 10 Ω. Voltage threshold values were set to 0.12 V and 0.32 V for U_{min} and U_{max}, respectively. The resulting profile of P_{av} is shown in Fig. 6A. It can be seen, that by intermittently connecting the electrical load based on the voltage threshold, the power output was maximized both under acetate non-limiting and non-limiting conditions without changing the value of the external resistance. The corresponding duty cycle values are shown in Fig. 6B. It can be seen that at a low acetate concentrations, the *D* values decreased, i.e. R_{ext} was connected for a shorter time during each cycle. Considering that for practical MFC application for electricity production MFC output voltage should be converted to at least 5 V, e.g. using an up-converter, this approach would also allow for better up-converter performance. Although up-converters can operate at low input voltages, the conversion efficiency decreases if the input voltage drops below 100 mV. For practical applications, the overall system efficiency can be improved by implementing the *D*-cycle control using pre-selected voltage thresholds and controlling the electrical load with a low resistance transistor and a comparator.

4. Conclusions

This study demonstrates that an MFC can be operated at electrical loads below the MFC internal resistance without significant energy losses and proposes a practical method for maximizing MFC power output. The problem of R_{ext} and R_{int} mismatch is resolved by MFC operation with periodic resistance connection, where the connection and disconnection times are controlled based on the voltage measurements. The proposed approach not only resolves the problem of resistance mismatch but also accounts for the changes in MFC electrochemical characteristics due to variations in operating conditions.

Acknowledgement

This work was supported by the National Research Council of Canada, NRC publication #53404.

References

[1] B.E. Logan, J.M. Regan, Trends Microbiol. 14 (2006) 512–518.
[2] D.R. Lovley, Nat. Rev. Microbiol. 4 (2006) 497–508.
[3] H. Rismani-Yazdi, S.M. Carver, A.D. Christy, I.H. Tuovinen, J. Power Sources 180 (2008) 683–694.
[4] R.A. Rozendal, H.V.M. Hamelers, K. Rabaey, J. Keller, C.J.N. Buisman, Trends Biotechnol. 26 (2008) 450–459.
[5] P. Aelterman, M. Versichele, M. Marzorati, N. Boon, W. Verstraete, Bioresour. Technol. 99 (2008) 8895–8902.
[6] L. Woodward, B. Tartakovsky, M. Perrier, B. Srinivasan, Biotechnol. Prog. 25 (2009) 676–682.
[7] B.E. Logan, Microbial Fuel Cells, John Wiley & Sons Inc., Hoboken, NJ, 2008.
[8] L. Woodward, M. Perrier, B. Srinivasan, R.P. Pinto, B. Tartakovsky, AIChE J. 56 (2010) 2742–2750.
[9] G.C. Premier, J.R. Kim, I. Michie, R.M. Dinsdale, A.J. Guwy, J. Power Sources 196 (2011) 2013–2019.
[10] T. Esram, P.L. Chapman, IEEE Trans. Energy Convers. 22 (2007) 439–449.
[11] E. Koutroulis, K. Kalaitzakis, IEEE Trans. Ind. Electron. 53 (2006) 486–494.
[12] B. Tartakovsky, M.F. Manuel, V. Neburchilov, H. Wang, S.R. Guiot, J. Power Sources 182 (2008) 291–297.
[13] R.P. Pinto, B. Srinivasan, S.R. Guiot, B. Tartakovsky, Wat. Res. 45 (2011) 1571–1578.
[14] Y. Fan, E. Sharbrough, H. Liu, Environ. Sci. Technol. 42 (2008) 8101–8107.
[15] S. Trasatti, O.A. Petrii, Pure Appl. Chem. 63 (1991) 711–734.
[16] S. Chen, G. He, A.A. Carmona-Martinez, S. Agarwal, A. Greiner, H. Hou, U. Schröder, Electrochem. Commun. 13 (2011) 1026–1029.
[17] C. Donovan, A. Dewan, D. Heo, H. Beyenal, Environ. Sci. Technol. 42 (2008) 8591–8596.